Patterns of genomic variation reveal a single evolutionary origin of the wild allotetraploid *Mimulus sookensis*

Single evolutionary origin of *M. sookensis*

Makenzie R. Whitener[1*], Hayley Mangelson[2], and Andrea L. Sweigart[1]

[1]Department of Genetics, University of Georgia, Athens, GA, 30602, USA
[2]Phase Genomics, Seattle, WA, USA

[*]Corresponding Author:
Makenzie Whitener
120 E. Green St.
Athens, GA 30602
makenzie.whitener@gmail.com

Data Accessibility

Whole genome sequence data of lines used will be deposited to the NCBI Sequence Read Archive upon acceptance. The *Mimulus sookensis* FAN v1 reference genome will be made publicly available.

Conflict of Interest

The authors declare no conflict of interests.

Abstract

Polyploidy occurs across the tree of life and is especially common in plants. Because newly formed cytotypes are often incompatible with their progenitors, polyploidy is also said to trigger "instantaneous" speciation. If a polyploid can self-fertilize or reproduce asexually, it is even possible for one individual to produce an entirely new lineage. How often this extreme scenario occurs is unclear, with most studies of wild polyploids reporting multiple origins. Here, we explore the evolutionary history of the wild allotetraploid *Mimulus sookensis*, which was formed through hybridization between self-compatible, diploid species in the *Mimulus guttatus* complex. We generate a chromosome-scale reference assembly for *M. sookensis* and define its distinct subgenomes. Despite previous reports suggesting multiple origins of this highly selfing polyploid, we discover patterns of population genomic variation that provide unambiguous support for a single origin, which we estimate occurred ~71,000 years ago. One *M. sookensis* subgenome is clearly derived from the selfer *M. nasutus*, which, based on organellar variation, also appears to be the maternal progenitor. The ancestor of the other subgenome is less certain, but it shares variation with both *M. decorus* and *M. guttatus*, two outcrossing diploids that overlap broadly with *M. sookensis*. Whatever its precise ancestry, this study establishes *M. sookensis* as an example of instantaneous speciation, likely facilitated by the polyploid's predisposition to self-fertilize. With a reference genome for *M. sookensis* now available and its origin clarified, this wild tetraploid is poised to become a model for understanding the genetic and evolutionary mechanisms of polyploid persistence.

Introduction

Polyploids are found across the tree of life and in nearly all extant flowering plant families (Jiao et al., 2011). This near ubiquity in angiosperms is likely due in part to the high incidence of polyploid formation (Barker et al., 2016; Herben et al., 2016; Kreiner et al., 2017; Ramsey, 2007), which is on the order of the mutation rate for autopolyploids (Ramsey & Schemske, 1998)but it might also be due to immediate and/or longer-term selective advantages of whole genome duplication (Comai, 2005). Nevertheless, the initial rarity of a newly formed polyploid (i.e., minority cytotype exclusion, Levin, 1975), combined with potentially strong reproductive isolation with its nearby progenitor species, presents a major challenge to establishment (Burton & Husband, 2000). One way to overcome this hurdle is self-fertilization (Rodriguez, 1996) and, indeed, polyploids are more likely to self than their diploid relatives (Barringer, 2007). In the extreme case of a single newly formed polyploid individual, its swift extinction is assured unless it can self-fertilize or backcross via a triploid bridge (Coyne & Orr, 2004; Ramsey & Schemske, 1998) – or unless there are other polyploid relatives nearby. Given this major constraint, it is perhaps not surprising that many polyploid species seem to have multiple evolutionary origins (reviewed in Soltis et al., 2014 and Soltis & Soltis, 1999). Even in self-fertilizing polyploids, which theoretically *can* evolve from a single individual, the high rate of unreduced gamete production (especially in F1 hybrids leading to allopolyploids, Ramsey & Schemske, 1998) might often facilitate multiple evolutionary origins.

After decades of studies reporting evidence of multiple evolutionary origins in diverse polyploid species (Abbott & Lowe, 2004; Allender & King, 2010; Doyle et al., 1990; Hegarty et al., 2012; Mavrodiev et al., 2015; Meimberg et al., 2009; Novikova et al., 2017; Segraves et al., 1999; Sigel et al., 2014; Vallejo-Marín et al., 2015; Wolfe et al., 2023; Zou et al., 2015), we might reasonably ask whether single-origin polyploidy is so rare as to be of little evolutionary

71 importance. Still, there are notable exceptions to the multiple-origin rule including wild and
72 cultivated species of peanut (*Arachis monticola* and *A. hypogaea*, Bertioli et al., 2019), *Coffea*
73 *arabica* (Scalabrin et al., 2020), and the invasive allododecaploid *Spartina anglica* (Ainouche et
74 al., 2004). It is also worth noting that most of what we know about the evolutionary origins of
75 *wild* polyploid species comes from early molecular studies with a limited number of markers
76 (Doyle et al., 1990; Hegarty et al., 2012; Mavrodiev et al., 2015; Segraves et al., 1999; Slotte et
77 al., 2006; Soltis & Soltis, 1999; Soltis & Soltis, 1991). In the only wild polyploid systems with
78 abundant population genomic data (species in *Arabidopsis* and *Capsella*), the question of
79 evolutionary origins has been challenging to resolve. For example, in *C. bursa-pastoris*, support
80 has been equivocal for multiple origins vs. a single origin with admixture from diploid relatives
81 (Douglas et al., 2015; Kryvokhyzha et al., 2019), though a recent discovery of an early
82 homeologous exchange event shared species-wide might provide evidence for the latter (Penin et
83 al., 2023). In the allotetraploid *A. suecica*, early evidence from microsatellite markers had
84 suggested a unique origin (Jakobsson et al., 2006), but more recent, whole-genome population
85 resequencing revealed extensive shared polymorphism with diploid progenitors, suggesting
86 multiple founding individuals (Novikova et al., 2017).
87 Given the technical challenges of phasing duplicated genomes, a reference assembly is an
88 indispensable tool for gaining insight into the evolutionary origins of a polyploid species.
89 However, it has been only recently that advances in long-read sequencing and chromatin
90 confirmation capture have enabled assembly of complex and repetitive polyploid genomes
91 (Michael & VanBuren, 2020). In polyploid crops, which include many species of major
92 economic importance, the last few years have seen a burst of genome assembly (Bertioli et al.,
93 2019; Borrill et al., 2015; Chen et al., 2020; Edger et al., 2019; Kamal et al., 2022; Scalabrin et

al., 2020). Still, *wild* polyploid systems have lagged behind – even though they are essential for understanding the ecological context and evolutionary mechanisms of polyploid formation, establishment, and persistence (Soltis et al., 2016).

The allotetraploid monkeyflower, *Mimulus sookensis*, is one such system, having formed recently through hybridization between diploid species in the well-studied *M. guttatus* species complex (Benedict et al., 2012; Sweigart et al., 2008). Studies of allozyme (Benedict 1993) and nucleotide sequence variation (Modliszewski & Willis, 2012; Sweigart et al., 2008) have pointed to *M. guttatus* and *M. nasutus* as the diploid progenitors of *M. sookensis*. These two closely related diploid species range across much of western North America (Figure S1), and in areas of secondary sympatry, historical and contemporary introgression is common – largely from *M. nasutus* into *M. guttatus* (Brandvain et al., 2014; Kenney & Sweigart, 2016; Sweigart & Willis, 2003; Zuellig & Sweigart, 2018). The two diploid species also overlap with *M. sookensis*, which has been sampled from Vancouver Island, British Columbia, Canada to California, USA (Figure S1).

Although the geographic overlap and ongoing hybridization of *M. guttatus* and *M. nasutus* seem to build a strong case for their status as progenitors of *M. sookensis*, several key questions about the evolutionary origin of this allotetraploid species remain. One is the number of times it has evolved. Using nucleotide sequence polymorphism to investigate genetic variation in natural populations of *M. sookensis*, an early study with only two nuclear loci suggested the species had at least two evolutionary origins (Sweigart et al., 2008). A few years later, with an additional six nuclear loci and three chloroplast loci, the estimate increased to 11 independent origins (Modliszewski & Willis, 2012). Paradoxically, the same study showed no evidence of postzygotic reproductive isolation among any *M. sookensis* lines, which might be expected with

multiple origins if duplicate gene copies are subject to divergent histories of degenerative mutation (Lynch & Force, 2000). Another question is the timing of the allotetraploid's evolutionary origin. With only a handful of loci, previous studies have not attempted to estimate when *M. sookensis* evolved.

A final outstanding question is whether *M. guttatus* is a true progenitor. Although support for *M. nasutus* as a progenitor is strong, evidence for *M. guttatus* is mixed. Phenotypically, *M. sookensis* is nearly identical to *M. nasutus* (Benedict et al., 2012); both species are highly selfing, with small, often cleistogamous flowers. *M. guttatus*, on the other hand, is a large-flowered, primarily outcrossing species, and F1 hybrids from crosses with *M. nasutus* show dominance in floral traits toward *M. guttatus* (Fishman et al., 2002). Genetically, too, there is a much closer match between *M. nasutus* and *M. sookensis*, with molecular studies invariably showing high sequence similarity between one *M. sookensis* gene copy and *M. nasutus* alleles (Benedict 1993; Modliszewski & Willis, 2012; Sweigart et al., 2008). Although these same studies also show sequence similarity between the alternative *M. sookensis* gene copies and *M. guttatus* alleles, the exceptionally high genetic diversity of *M. guttatus* (Brandvain et al., 2014; Puzey et al., 2017) makes it nearly impossible to identify a direct progenitor. Even *M. nasutus* carries only a subset of the genetic variation present in *M. guttatus*, and the two species have very few fixed differences (Brandvain et al., 2014; Sweigart & Willis, 2003). In addition to *M. guttatus* and *M. nasutus*, the species complex includes several other closely related, often interfertile species (Vickery, 1978). Most of these species are unlikely progenitors, as they have restricted geographic distributions well outside the range of *M. sookensis*. However, one of them – *M. decorus* – is an outcrossing species with a range that largely overlaps both *M. nasutus* and *M. sookensis* (Figure S1).

In this study, we generate and leverage a new, chromosome-scale reference genome assembly for *M. sookensis* to clarify the details of its evolutionary history. Using whole genome sequence data (WGS) from *M. sookensis* accessions collected from across the species range, we perform population genomic analyses to determine the number and timing of evolutionary origins. We also revisit the question of ancestry, taking advantage of published WGS data from diverse *M. guttatus* complex accessions to identify the likely progenitors of *M. sookensis*. With these new genomic resources for *M. sookensis*, we expect this species to become a model for understanding the ecological context and genetic mechanisms of polyploid evolution.

Methods

Plant material, molecular methods, and sequencing

To generate plant material for the *M. sookensis* reference assembly, we grew a single plant from selfed seed of FAN36, an accession originally collected on Vancouver Island in British Columbia, Canada (Table S1). Because wild *M. sookensis* is primarily selfing, the FAN36 line is highly inbred and homozygous. This plant was grown in the University of Georgia Botany greenhouses in a 4-in pot with moist Fafard 4P growing mix (Sun Gro Horticulture, Agawam, MA) under 16-h days at 23°C and 8-h nights at 16°C. Once the plant had grown to a large size with several branches, we shipped it to Phase Genomics (Seattle, WA) for high-molecular weight DNA extraction, PacBio sequencing, and Hi-C chromatin capture.

Phase Genomics used ~250 mg of leaf tissue from FAN36 to perform DNA extraction with the Qiagen MagAttract HMW DNA kit. Libraries were prepared using a PacBio Sequel II Binding Kit 2.2 and sequenced on a PacBio Sequel IIe instrument, producing 1,639,773 CCS HiFi reads with a total length of 24.27 Gb (average read length: 14.8 kb). Chromatin

conformation capture data were generated using the Phase Genomics Proximo Hi-C 3.0 Kit, which is a commercially available version of the Hi-C protocol (Lieberman-Aiden et al., 2009). The resulting library was sequenced on an Illumina HiSeq 4000, generating a total of 242,673,575 150-bp PE reads.

We used new and previously generated whole genome sequence (WGS) data from 11 wild *M. sookensis* accessions collected from 10 populations across the species range (Table S1). Selfed seeds for each accession were grown as for FAN36 above. We performed DNA extractions using a CTAB-chloroform protocol (Fishman 2020) on bud and leaf tissue. DNA was submitted to Duke Center for Genomic and Computational Biology for sequencing where 150-bp PE reads were generated on an Illumina NovaSeq 6000 S1 lane.

Genome assembly and annotation

To generate contigs for the *M. sookensis* assembly, we assembled the FAN36 HiFi reads with hifiasm v0.19.3 (Cheng et al., 2021) using the -l0 parameter to skip purging and preserve homoeologous regions. This method resulted in an initial assembly of 748 Mb with 3,671 contigs (N50 = 0.96 Mb). Evaluation of this assembly with KRAKEN v2.1.1(Wood et al., 2019) showed evidence of microbial contamination. Subsequent investigation with ProxiMeta (Press et al., n.d.; Stewart et al., 2018) to perform metagenome deconvolution, CheckM, v1.0.11 (Parks et al., 2015) to assess quality, and Mash v1.1.1 (Ondov et al., 2016) to determine taxon identity, revealed the inclusion of 32 microbial genome clusters. Removing all prokaryotic sequences from the initial contig assembly resulted in a draft assembly of 590 Mb with 979 contigs (N50 = 1.19 Mb).

To generate chromosome-scale scaffolds, we mapped Hi-C reads to the draft assembly following the Phase Genomics Proximo Hi-C Kit recommendations (https://phasegenomics.github.io/2019/09/19/hic-alignment-and-qc.html). Briefly, we aligned reads using BWA-MEM v0.7.17 (Li & Durbin, 2010) with the -5SP and -t 8 options specified and all other options default. We flagged PCR duplicates (later excluded from the analysis) using SAMBLASTER v0.7.17 (Faust & Hall, 2014) and filtered alignments using SAMtools v1.9 (Danecek et al., 2021) with the -F 2304 filtering flag to remove non-primary and secondary alignments. To create scaffolds, we used a single-phase procedure first used in Bickhart et al., 2017. As in the LACHESIS method (Burton et al., 2013), this procedure computes a contact frequency matrix from the aligned Hi-C read pairs (normalized by the number of Sau3AI restriction sites on each contig) and constructs scaffolds to optimize expected contact frequency in Hi-C data. We used Proximo to perform ~20,000 iterations of this dataset to optimize the number of scaffolds, as well as the orientation and order of contigs (maximizing concordance with the observed Hi-C data). Using Juicebox v0.7.17 (Durand et al., 2016; Rao et al., 2014) to manually correct scaffolding errors produced a final, 574-Mb *M. sookensis* FAN v1 assembly that includes 28 chromosome-scale scaffolds ranging in size from 10.18 Mb to 26.69 Mb (the assembly also includes a 5-Mb scaffold with sequences that could not be assembled into the main chromosome-level scaffolds.). A 15 Mb fungal contaminant identified via NCBI BLAST (blast.ncbi.nlm.nih.gov, Altschup et al., 1990) was removed from the assembly. We used BUSCO v5.2.2 (Simão et al., 2015) in genome mode with eukaryota odb10 to evaluate the completeness of the assembly.

To generate a preliminary annotation for the *M. sookensis* FAN v1 reference, we used Liftoff v1.6.3 (Shumate & Salzberg, 2021) and the *M. guttatus* v3 annotation (phytozome.org).

Because *M. sookensis* should contain twice the number of genes as its diploid progenitor, we used the *-copies* flag along with *-sc 0.75* to ensure high quality lift over.

Subgenome identification

To identify homeologous chromosome pairs, we performed genome comparisons between *M. sookensis* and its presumed diploid progenitors. We used MiniMap2 v2.26 (Li, 2018) to compare the *M. sookensis* FAN v1 genome to the *M. guttatus* IM62 v3 and *M. nasutus* SF v1 reference assemblies (phytozome.org) and generated dot plots using dotPlotly (Tom Poorton, https://github.com/tpoorten/dotPlotly).

We assigned subgenomes by mapping previously generated WGS from *M. nasutus* SF (Table S1) to the *M. sookensis* FAN v1 assembly. We used TRIMMOMATIC v0.36 (Bolger et al., 2014) to remove adapters, BWA-mem v0.7.17 (Li, 2013; Li & Durbin, 2010) to align SF to FAN v1, and Picard v2.27.4 (http://broadinstitute.github.io/picard) to add read groups and remove optical and PCR duplicates. We then filtered reads for MQ > 28 in SAMtools v1.16.1 (Danecek et al., 2021). To calculate SF *M. nasutus* read coverage across the *M. sookensis* FAN v1 assembly, we used the coverage tool in SAMtools (Danecek et al., 2021). Additionally, to assess SF-FAN sequence similarity, we generated a VCF file using the mpileup and call tools from BCFtools v1.15.1(Danecek et al., 2021). We used VCFtools v0.1.16 (Danecek et al., 2011) to remove indels and include only biallelic sites with quality > 29. We filtered each VCF to include only sites with read depth ≥10 and <mean+2*stdev. We used Pixy v1.27.beta1 (Korunes & Samuk, 2021) to calculate nucleotide diversity (π) between FAN and SF.

We used MiniMap2 v2.26 and Circos v0.69 (Krzywinski et al., 2009) to visualize regions of homeology in the *M. sookensis* genome. To explore synteny across the genome between *M.*

sookensis and putative progenitors, we input peptide fasta and gff files for *M. sookensis* FAN v1, *M. guttatus* IM62 v3, and *M. nasutus* SF v1 into GENESPACE v1.2.3 (Lovell et al., 2022).

Population genomic analyses

To investigate patterns of natural variation in *M. sookensis*, we aligned WGS data from 11 wild accessions (Table S1) to the *M. sookensis* FAN v1 reference assembly using the methods described above for SF *M. nasutus*. Using the mpileup and call tools from BCFtools v1.15.1 (Danecek et al., 2021), we generated a VCF for each accession. We used VCFtools v0.1.16 (Danecek et al., 2011) to remove indels and include only biallelic sites with quality > 29. We filtered each VCF to include only sites with read depth ≥10 and <mean+2*stdev and 80% of individuals were genotyped. We performed a principal component analysis (PCA) in R [4.1.3] (R core team 2021) using the package "SNPRelate" (Zheng et al., 2012). To visualize the axes, we used ggplot2 (Wickham H, 2016) in R. We used Pixy v1.27.beta1 (Korunes & Samuk, 2021) to calculate heterozygosity and π. For these and all downstream analyses, we took advantage of having Illumina WGS data from the same FAN36 accession used to generate the reference assembly. To minimize problematic alignments caused by assembly errors, we excluded reads from any of the 11 wild *M. sookensis* lines that mapped to genomic regions where FAN36 itself was identified as heterozygous.

To perform genome comparisons between *M. sookensis* and its potential diploid progenitors, we separated *M. sookensis* into its two subgenomes. We aligned the 11 wild accessions to the FAN v1 reference using BWA-mem v0.7.17 (Li & Durbin, 2010), split resulting BAM files by chromosome, and merged the split BAM files using SAMtools v1.16.1 merge (Danecek et al., 2021) into separate files representative of the subgenomes. We then

converted BAM files back to the FASTQ format using SAMtools v1.16.1 bam2fq (Danecek et al., 2021). We aligned the separate subgenomes of 11 *M. sookensis* to the *M. guttatus* v5 reference assembly, along with previously generated WGS from *M. guttatus*, *M. nasutus*, *M. decorus*, and a *M. dentilobus* accession as an outgroup (Table S1). Using GATK v3.8-1 HaplotypeCaller with the -allSites flag (McKenna et al., 2010) we generated a VCF. We removed indels and used only biallelic sites with read depth ≥10 and < mean+2*stdev that passed the following filters: mapping quality (MQ) > 30, mapping quality rank sum (MQRankSum) > -12.5, fisher strand (FS) < 60, quality depth (QD) > 2, quality (QUAL) > 30 and read position rank sum (ReadPosRankSum) > -8. Additionally, we filtered individual VCF files for each sample to include only sites with read depth ≥ 3 and < mean+2*stdev. We used VCFtools v0.1.16 (Danecek et al., 2011) to remove sites with > 20% missing data.

From this dataset, we generated neighbor joining (NJ) and maximum likelihood (ML) trees that included all 22 *M. sookensis* subgenomes, as well as closely related diploid species in the *M. guttatus* complex to investigate the evolutionary history of *M. sookensis*. In R, we used the package “ape” to construct the NJ tree and “phangorn” to perform 1000 bootstraps on a downsampled dataset of 14,000 SNPs. After conversion into PHYLIP format with custom scripts from Simon Martin (https://github.com/simonhmartin/genomics_general/tree/master), we generated the ML tree with the full dataset using IQ-Tree v2.2.0 (Nguyen et al., 2015) with TVM+F+R2 as the best fit model. The ML tree included 3,576,989 (1,711,738 parsimony informative) sites. Finally, we identified fourfold degenerate sites using a custom script (Tim Sackton: https://github.com/tsackton/linked-selection/tree/master/misc_scripts) and then used a python script (Note S1 in Garner et al., 2016) to calculate nucleotide diversity (π_{sil}) and divergence (d_{xy}) among samples.

To characterize variation in species relationships across the genome, we used IQ-Tree v2.2.0 to generate 16,754 gene trees including only genes with variant calls for all taxa. For each gene, we used BCFtools v1.15.1(Danecek et al., 2021) consensus to generate a concatenated fasta and the seqtk v1.3 'randbase' tool (https://github.com/lh3/seqtk) to randomly select one allele at heterozygous sites. Next, we used TWISST v0.2 (Martin & Van Belleghem, 2017) in two separate analyses to quantify support for particular (rooted) gene tree topologies given a specified set of species in the dataset. In the first analysis, we excluded *M. sookensis* samples and grouped the remaining diploids into three "species": *M. decorus*, northern *M. guttatus*, and southern *M. guttatus* + *M. nasutus*. We quantified support for each of the three possible gene tree topologies with *M. dentilobus* as the outgroup. Our rationale for combining southern *M. guttatus* and *M. nasutus* into one "species" and for separating *M. guttatus* into two was that these groupings form well-supported clades with whole genome data (Brandvain et al., 2014, also see Results). Moreover, because our intent with this analysis was to investigate whether discordant gene trees might help explain conflicting whole-genome tree topologies that have alternatively placed *M. decorus* within northern *M. guttatus* (Coughlan et al., 2020; Ivey et al., 2023) or sister to all of *M. guttatus* (Coughlan and Willis 2019), it was necessary to distinguish between geographic clades. In the second TWISST analysis, we included *M. sookensis* subgenomes and quantified support for one or more diploid relatives as a likely progenitor. In this analysis, we categorized the 105 rooted gene tree topologies (for five taxa plus *M. dentilobus* as an outgroup) into simplified "classes" defined by sister groupings between a focal *M. sookensis* subgenome and the diploid taxa. We also visualized genome-wide support for the most frequent of these topology classes by averaging topology weights in non-overlapping nine-gene windows.

To attempt to identify the maternal progenitor of *M. sookensis*, we characterized patterns of variation in the chloroplast and mitochondrial genomes. Using BWA-mem v07.17 (Li & Durbin, 2010) we aligned WGS from 11 *M. sookensis, 20 M. guttatus, 8 M. decorus, and 5 M. nasutus* to an *M. guttatus* IM62 mitochondria assembly (Mower et al., 2012), excluding regions annotated as derived from the chloroplast. We also aligned the same WGS data to the chloroplast genome of the *M. guttatus* IM767 v1 reference assembly (phytozome.org). Using the mpileup and call tools from BCFtools v1.15.1(Danecek et al., 2021), we generated a combined VCF for each genome and used VCFtools v0.1.16 (Danecek et al., 2011) to remove indels and include only biallelic sites with quality > 29. We excluded sites with heterozygous calls or with any missing data. For each organellar genome, we constructed a haplotype network using PopArt (Leigh & Bryant, 2015). The mitochondrial network used 233 sites (100 parsimony informative) and the chloroplast network used 181 sites (91 parsimony informative).

Results

Mimulus sookensis genome assembly

Consistent with its status as an allotetraploid, the *M. sookensis* genome assembly is 574 Mb, roughly twice the size of the reference genomes of closely related diploids (*M. guttatus* IM62 v3 = 339.2 Mb, *M. nasutus* SF v3 = 312.8 Mb, phytozome.org). Additionally, we recovered 28 chromosome-scale scaffolds in *M. sookensis* (Figure S2), double the base number of chromosomes in the group (Mukherjee & Vickery, 1962). Both synteny mapping and homology between *M. sookensis* and its diploid relatives show that each of the 14 chromosomes in *M. nasutus* and *M. guttatus* corresponds to exactly two chromosomes in *M. sookensis* (Figure 1, Figure S3). This sequence homology spans chromosomes end-to-end indicating there have

been no large-scale deletions or chromosome loss in *M. sookensis*. We do find evidence of a *M. sookensis* specific inversion at the tip of chromosome 14 of subgenome A. Finally, BUSCO analysis revealed the new *M. sookensis* FAN v1 assembly to be 98.2% complete and, consistent with a recent whole genome duplication, 90.2% of BUSCOs are duplicated (C:98.4% [S:8.2%, D:90.2%], F:0.5%, M:1.1%, n:2326).

Subgenome identification

To define subgenomes, we aligned WGS from *M. nasutus* SF to the *M. sookensis* FAN v1 reference, reasoning that sequence from this putative progenitor should match only one set of 14 chromosomes. Indeed, for each pair of *M. sookensis* homeologs, *M. nasutus* read depth was much higher on one chromosome than on the other (Table 1). Using this analysis, we defined the set of 14 chromosomes with higher *M. nasutus* coverage as subgenome A (average read depth = 6.2) and the set with lower *M. nasutus* coverage as subgenome B (average read depth = 0.55). Nucleotide diversity is much lower when *M. nasutus* is compared to subgenome A (π = 0.005) than subgenome B (π = 0.025) and is also similar to nucleotide diversity within *M. nasutus* (π = 0.014: Garner et al., 2016). Taken together, these results point to *M. nasutus* as the progenitor of subgenome A but not subgenome B. The two subgenomes show little to no sequence synteny outside homeologous pairs (Figure S4).

Evolutionary origin of sookensis

Despite sampling *M. sookensis* from locations spanning most of its range, we detected little population structure in this species with PCA revealing no distinction between northern and southern populations (Figure 2). Additionally, we discovered very little genetic variation in *M. sookensis*: average pairwise nucleotide diversity (π) is only 0.0045 ~half that of its selfing

progenitor (*M. nasutus*). These results are strong evidence of a single evolutionary origin of *M. sookensis*.

To investigate this origin more deeply, we separated *M. sookensis* into its two subgenomes for comparisons with diploid relatives in the *M. guttatus* complex. Consistent with a single allopolyploid origin, the two *M. sookensis* subgenomes form distinct monophyletic groups in maximum likelihood (Figure 3, Figure S6) and neighbor-joining (Figure S5) trees. The subgenome A samples are nested within the *M. nasutus* clade, confirming this species as a progenitor of *M. sookensis*. The identity of the other progenitor, however, is less certain. In contrast to previous studies (Modliszewski & Willis, 2012; Sweigart et al., 2008), which focused exclusively on *M. nasutus* and *M. guttatus* as potential progenitors (and did not include analyses of any other diploid relatives), we discovered that subgenome B clusters most closely with *M. decorus* (Figure 3, Figure S5). However, unlike with subgenome A, we did not observe the nested pattern of variation expected for a direct progenitor. We note there is extensive hybridization and incomplete lineage sorting among closely related members of the *M. guttatus* complex (Brandvain et al., 2014), which complicates phylogenetic reconstructions, and *M. decorus* has alternatively been placed within the northern *M. guttatus* clade (Coughlan et al., 2021; Ivey et al., 2023) and outside of *M. guttatus* altogether (this study, Coughlan & Willis, 2019). Even with this uncertainty about the identity of one progenitor, the pattern of variation – with each subgenome forming a well-supported, distinct clade – provides unambiguous support for a single evolutionary origin of *M. sookensis*. Moreover, assuming this origin arose through a single F1 individual, we can estimate it occurred only ~71,000 years ago (with time of origin $T \sim \pi_{sil}/\mu$ and π_{sil} = 0.011 = average π_{sil} of subgenome A and B [Table S2], assuming $\mu = 1.5\times10^{-8}$ following Brandvain et al., 2014).

We next used TWISST (Martin & Van Belleghem, 2017) to quantify support for alternative evolutionary histories across the genome. In an initial analysis excluding *M. sookensis* (Figure S7), we discovered that gene tree topologies with *M. decorus* outside of *M. guttatus* are only slightly more common (~43%) than topologies with *M. decorus* sister to northern *M. guttatus* (~33%). Next, in an analysis with the full taxon dataset, we quantified support for one or more diploid species as the closest relative of *M. sookensis* subgenome B. We defined five "species" in this analysis (in addition to *M. dentilobus* as the outgroup): *M. sookensis* subgenome B, *M. decorus*, northern *M. guttatus*, southern *M. guttatus*, and *M. nasutus* + *M. sookensis* subgenome A. Our rationale for collapsing *M. nasutus* and subgenome A into a single species was that these samples form a well-supported clade in the whole-genome tree (Figure 3) and it reduces the number of tree topologies to a manageable number. We categorized the 105 rooted gene tree topologies into simplified classes defined by sister groupings between *M. sookensis* subgenome B and all possible combinations of the four other diploid species (Figure 4, Figure S8). The most common class of topologies have *M. decorus* as sister to subgenome B (~36%), mirroring the whole-genome species tree (Figure 3). This relationship occurs more than twice as often as the second most common class of topologies (subgenome B equally related to *M. decorus*, *M. guttatus*, and *M. nasutus*: ~15%) and more than three times the third most common class (subgenome B sister to northern *M. guttatus*: ~11%). Across the genome, there is alternating support for these top three topology classes (Figure S9), with little evidence of recent introgression (i.e., large contiguous blocks supporting a particular topology) from any of these diploid species into *M. sookensis*. The fourth most common topology class (~8%) places subgenome B as sister to the *M. nasutus*/subgenome A group (Figure 4, Figure S10), which

might be due to gene conversion and/or homeologous recombination between the *M. sookensis* subgenomes.

Finally, in an attempt to identify the maternal progenitor of *M. sookensis*, we analyzed patterns of variation in mitochondrial and chloroplast genomes. Although previous analyses with fewer loci and taxa found no species-diagnostic haplotypes in the *M. guttatus* complex (Modliszewski & Willis, 2012; Vallejo-Marín et al., 2016), both organellar genomes in this study revealed structure between species. In both the mtDNA and cpDNA haplotype networks, *M. nasutus* and *M. sookensis* cluster together in a group that also includes four *M. guttatus* samples (Figure 5). Taken at face value, this result might suggest that shared variation between diploid relatives precludes identification of the *M. sookensis* maternal progenitor. However, three of the four *M. guttatus* accessions in this group are from populations with ongoing introgression from *M. nasutus* (Brandvain et al., 2014; Kenney & Sweigart, 2016). This fact, together with the finding that almost all *M. decorus* samples cluster separately (except for one sample – LL – that groups with *M. sookensis* only in the mtDNA network) suggests that *M. nasutus* is the maternal progenitor of *M. sookensis*.

Discussion

Understanding why polyploidy is so ubiquitous across the angiosperm phylogeny requires a focus on wild systems. Here, we generate a chromosome-scale reference genome assembly for the wild allotetraploid *Mimulus sookensis*, which formed through hybridization between closely related yellow monkeyflower species in the *M. guttatus* complex. This new genome assembly allowed us to interrogate the evolutionary history of *M. sookensis*, providing definitive evidence of a single origin of the species, which we estimate occurred ~71,000 years

ago. Additionally, our analysis defined the two distinct subgenomes of *M. sookensis*, one of which is clearly derived from the diploid selfing species, *M. nasutus*. Going forward, this new genome will be an invaluable resource for understanding the genetic mechanisms of adaptation in *M. sookensis*, as well as divergence from its progenitors.

Single origin of M. sookensis

Our discovery that *M. sookensis* has a single evolutionary origin differs dramatically from previous work suggesting as many as 11 origins (Modliszewski & Willis, 2012). How do we explain this large discrepancy? Inference in the earlier study was based on nucleotide sequence variation at a much more limited number of loci (8 nuclear, 3 chloroplast), only two of which showed truly high levels of polymorphism consistent with multiple origins (Modliszewski & Willis, 2012). In light of our genome-wide data, which clearly show low variability in *M. sookensis* across most of the genome (π = 0.0045), these two loci appear to be outliers. Indeed, we reexamined sequence variation at these two loci (*Mg1* and *Mg5*: Modliszewski & Willis, 2012) in our WGS dataset and found the same unusually high levels of polymorphism. This cause of high variation at these two loci is unknown but could be due to hybridization with other polyploid relatives in the *M. guttatus* complex (see below).

Like in *M. sookensis*, the availability of genome-wide sequence data and/or reference genomes has recently overturned or clarified the origin stories of several other wild and domesticated polyploid species. A high-quality reference genome for *Capsella bursa-pastoris*, for instance, helped uncover evidence of a homeologous exchange event that appears to have evolved very early in the species' evolutionary history (the exchange is geographically widespread and present in all studied accessions), suggesting that one origin with subsequent

introgression from diploid progenitors might be more likely than multiple origins (Penin et al., 2023). In *Arabidopsis suecica*, the story is reversed with multiple origins now inferred from extensive shared variation with its diploid progenitors (Novikova et al., 2018), instead of the single origin suggested by earlier studies of microsatellite variation (Jakobsson et al., 2006) In crops too, recent genomic analysis has begun to clarify what are often very complex evolutionary origins involving multiple rounds of hybridization between several different progenitors (e.g., bread wheat: Liu et al., 2022; Pont et al., 2019).

For several reasons, the finding of a single evolutionary origin of *M. sookensis* is somewhat surprising. One is simply a lack of precedent: among the wild polyploid species that have been studied, multiple origins seem to be the rule (Soltis et al., 2014, 2016; Soltis & Soltis, 1999; Another is that there might be ample opportunity for polyploid formation, with considerable historical and contemporary hybridization between some diploid species of the *M. guttatus* complex (Brandvain et al., 2014; Sweigart & Willis, 2003). Given the recent origin of *M. sookensis* and its fairly wide geographic distribution (at least from northern California to southern British Columbia), the hypothesis of multiple origins seems entirely plausible. On the other hand, that fact that *M. sookensis* was immediately able to self-fertilize when formed (one progenitor – *M. nasutus* – is a selfer and all *Mimulus* species are self-compatible) was likely a huge boon to its establishment (Fowler & Levin, 2016; Soltis et al., 2014) and might also have aided in its spread (Razanajatovo et al., 2016; Wright et al., 2013).

Search for the diploid progenitors

In line with previous evidence (Benedict et al., 2012; Sweigart et al., 2008), our study clearly identifies *M. nasutus* as a progenitor of *M. sookensis*. With the new *M. sookensis* FAN

genome assembly in hand, we were able to identify the set of 14 chromosomes derived from *M. nasutus*, which we call subgenome A. Additionally, by analyzing variants across the entire mitochondrial and chloroplast genomes, our study provides the strongest evidence to date of *M. nasutus* as the maternal progenitor. Due to extensive shared variation in the *M. guttatus* complex, previous studies of these genomes, which included either fewer loci (Modliszewski & Willis, 2012) or taxa (Vallejo-Marín et al., 2016), provided little resolution to distinguish among potential maternal progenitors. In this study, however, we find a consistent group of taxa that clusters together in both organellar networks; the group includes all *M. sookensis* samples, all *M. nasutus* samples, and four *M. guttatus* samples (plus one *M. decorus* sample in the mitochondrial network). Although, at first glance, this pattern seems to suggest shared variation in the diploid progenitors, three of the four *M. guttatus* samples that cluster in this group are from populations sympatric with *M. nasutus*, where extensive directional introgression (from *M. nasutus* into *M. guttatus*) has been documented (Brandvain et al., 2014; Kenney & Sweigart, 2016; Sweigart & Willis, 2003). Thus, it appears that hybridization in these sympatric populations may have resulted in organellar capture as has recently been found in other *Mimulus* species (Nelson et al., 2021). Moreover, these results build on previous intuition that, given the strong triploid block between *M. sookensis* and its diploid relatives (Sweigart et al., 2008), initial formation likely occurred via unreduced gametes in an F1 hybrid with *M. nasutus* as the seed parent.

Despite our extensive population genomic sampling, the identity of the second progenitor to *M. sookensis* remains somewhat mysterious. Although subgenome B clusters most closely with *M. decorus*, we do not observe the nested pattern of variation expected for a direct progenitor. Casting further doubt on *M. decorus* ancestry, the new genome assembly indicates that neither of the *M. sookensis* homeologs to chromosome 8 has the *DIV1* inversion (Figure S3),

482 which is carried by all perennial ecotypes of *M. guttatus* (Lowry & Willis, 2010; Oneal et al.,
483 2014) and is also found in perennial *M. decorus* (Coughlan and Willis 2019). Patterns of
484 sequence variation in the *DIV1* inversion suggest it is not new (Twyford and Friedman 2015) and
485 its presence in *M. decorus* suggest it evolved prior to this species' split with *M. guttatus* ~230
486 KYA (Coughlan & Willis, 2019). Thus, the recent origin of *M. sookensis* ~71 KYA seems to rule
487 out as a progenitor any species fixed for the *DIV1* inversion.

488 It should be noted that *M. guttatus* remains a candidate progenitor, as this species is
489 exceptionally diverse (Brandvain et al., 2014; Puzey et al., 2017) and has a large geographic
490 range that overlaps with *M. sookensis* and *M. nasutus*. Moreover, in at least three populations,
491 the three species currently co-occur (ROG and NHI; Sweigart et al., 2008; Catherine Creek,
492 unpublished results). Still, the fact that subgenome B of *M. sookensis* clusters outside of the *M.*
493 *guttatus* clade (Figure 3) suggests the polyploid carries ancestry either from unsampled *M.*
494 *guttatus* lineages or from other close relatives in the species complex. This ancestry might have
495 been present in *M. sookensis* from the start (derived from the original progenitor) or it might
496 have been introduced later through hybridization with close relatives. High sequence similarity
497 with *M. nasutus* across the entirety of subgenome A seems to suggest a primary influence of the
498 former, as evidence of hybridization should be found in both subgenomes. Additionally, patterns
499 of shared variation between subgenome B and its diploid relatives (*M. guttatus* and *M. decorus*)
500 are relatively constant across the genome (Figure S9) instead of blocky as might be expected
501 under a scenario of recent hybridization (Brandvain et al., 2014).

502 One intriguing possibility is that the unidentified progenitor could be another tetraploid in
503 the *M. guttatus* complex. Although there are no other widely distributed polyploids in the
504 complex, there have been reports of locally distributed *M. guttatus* autopolyploids (Vickery,

1995) and *M. decorus*-like polyploids (Coughlan et al. 2020), both of which overlap geographically with *M. sookensis* and *M. nasutus*. To investigate sequence similarity between *M. sookensis* and the *M. decorus*-like polyploid (which is a putative allotetraploid between *M. decorus* and an unknown species: J. Coughlan, pers. comm.), we aligned publicly available WGS from two accessions of this taxon (Table S1) to the *M. sookensis* FAN genome assembly. Contrary to the expectation if this *M. decorus*-like polyploid was a direct progenitor of subgenome B, we found similar sequence coverage across both *M. sookensis* subgenomes (A: 43.88%, B:56.69%). Future sampling efforts should target other, locally distributed polypoid taxa in the *M. guttatus* complex toward the goal of gaining additional insight into *M. sookensis* ancestry.

Conclusions and future directions

Our analyses of population genomic variation in *M. sookensis* provide definitive evidence of the species' recent and unique evolutionary origin. Although the direct progenitor of subgenome B remains somewhat mysterious, it is likely to have been an outcrosser, as other selfing species in the complex do not overlap with *M. sookensis*. One of the most salient features of *M. sookensis* is its nearly identical phenotype to *M. nasutus* (Benedict et al., 2012; Sweigart et al., 2008) and a key question in this system is what genetic mechanisms drive this similarity. Our finding of two distinct subgenomes corroborates previous studies of marker variation (Modliszewski & Willis, 2012; Sweigart et al., 2008), which have shown *M. sookensis* acts like a "fixed heterozygote," carrying gene copies from each of its progenitors. Although these intact subgenomes suggest there has not been large-scale homoeologous recombination, we do find a signal of local genomic similarity between subgenomes A and B, with the two subgenomes

clustering together in ~8% of gene trees (Figure S10). This sequence similarity is distributed across much of the genome and might indicate a history of gene conversion, but whether this mechanism results in the fixation of *M. nasutus* alleles in *M. sookensis* or explains the phenotypic resemblance of these two species remains to be seen. The new *M. sookensis* genome assembly also reveals a putative inversion at the end of chromosome 14A (Fig S3), which might be unique to the allotetraploid given that it has not been seen in the genomes of its diploid relatives (phytozome.org). With the origin of *M. sookensis* now clarified, and a new genome assembly available for this wild polyploid model system, we are now poised to address longstanding questions about the genetic and evolutionary mechanisms of polyploid establishment and spread.

Author Contributions

MRW and ALS designed and conceived the research. HM generated the assembly and Hi-C scaffolding and wrote the text related to these methods. MRW collected and analyzed the data. MRW and ALS wrote the manuscript.

Data Accessibility

Whole genome sequence data of lines used will be deposited to the NCBI Sequence Read Archive upon acceptance. The *Mimulus sookensis* FAN v1 reference genome will be made publicly available.

Acknowledgements

We thank J. Modliszewski and J. Willis who kindly provided seeds and shared whole genome sequence data for *M. sookensis*. We also thank J. Coughlan for sharing sequence data for *M. decorus*. We are grateful to J. Burke, J. Coughlan, K. Dyer, M. Farnitano, N. Gonzalez, J. Leebens-Mack, J. Modliszewski, S. Mantel, R. Schmitz, G. Sandstedt, VA. Sotola for helpful discussions. S. Mantel, M. Farnitano, and N. Gonzalez provided valuable feedback on the manuscript. This work was supported by an SSE Lewontin Award to MRW, a UGA Plant Center award to MRW, a Robin Hightower Genetics Graduate Support Fund award to MRW, and National Science Foundation grants IOS-1827645 and DEB-1856180 to ALS.

Conflict of Interest

The authors declare no conflict of interests.

561 Abbott, R. J., & Lowe, A. J. (2004). Origins, establishment and evolution of new polyploid
562 species: Senecio cambrensis and S. eboracensis in the British Isles. In *Biological Journal of*
563 *the Linnean Society* (Vol. 82).
564 https://academic.oup.com/biolinnean/article/82/4/467/2643079
565 Ainouche, M. L., Baumel, A., & Salmon, A. (2004). Spartina anglica C. E. Hubbard: A natural
566 model system for analysing early evolutionary changes that affect allopolyploid genomes.
567 *Biological Journal of the Linnean Society*, *82*(4), 475–484. https://doi.org/10.1111/j.1095-
568 8312.2004.00334.x
569 Allender, C. J., & King, G. J. (2010). *Origins of the amphiploid species Brassica napus L.*
570 *investigated by chloroplast and nuclear molecular markers* (Vol. 10).
571 http://www.biomedcentral.com/1471-2229/10/54
572 Altschup, S. F., Gish, W., Miller, W., Myers, E. W., & Lipman, D. J. (1990). Basic Local
573 Alignment Search Tool. In *J. Mol. Biol* (Vol. 215).
574 Barker, M. S., Arrigo, N., Baniaga, A. E., Li, Z., & Levin, D. A. (2016). On the relative
575 abundance of autopolyploids and allopolyploids. In *New Phytologist* (Vol. 210, Issue 2, pp.
576 391–398). Blackwell Publishing Ltd. https://doi.org/10.1111/nph.13698
577 Barringer, B. C. (2007). Polyploidy and self-fertilization in flowering plants. *American Journal*
578 *of Botany*, *94*(9), 1527–1533. https://doi.org/10.3732/ajb.94.9.1527
579 Benedict, B. G. (1993). *BIOSYSTEMATICS OF THE ANNUAL SPECIES OF THE Mimulus*
580 *guttatus SPECIES COMPLEX IN BRITISH COLUMBIA, CANADA*.
581 Benedict, B. G., Modliszewski, J. L., Sweigart, A. L., Martin, N. H., Ganders, F. R., & Willis, J.
582 H. (2012). Mimulus sookensis (Phrymaceae), a new Allotetraploid Species Derived from
583 Mimulus guttatus and Mimulus nasutus. *Madroño*, *59*(1), 29–43.
584 https://doi.org/10.3120/0024-9637-59.1.29
585 Bertioli, D. J., Jenkins, J., Clevenger, J., Dudchenko, O., Gao, D., Seijo, G., Leal-Bertioli, S. C.
586 M., Ren, L., Farmer, A. D., Pandey, M. K., Samoluk, S. S., Abernathy, B., Agarwal, G.,
587 Ballén-Taborda, C., Cameron, C., Campbell, J., Chavarro, C., Chitikineni, A., Chu, Y., …
588 Schmutz, J. (2019). The genome sequence of segmental allotetraploid peanut Arachis
589 hypogaea. *Nature Genetics*, *51*(5), 877–884. https://doi.org/10.1038/s41588-019-0405-z
590 Bickhart, D. M., Rosen, B. D., Koren, S., Sayre, B. L., Hastie, A. R., Chan, S., Lee, J., Lam, E.
591 T., Liachko, I., Sullivan, S. T., Burton, J. N., Huson, H. J., Nystrom, J. C., Kelley, C. M.,
592 Hutchison, J. L., Zhou, Y., Sun, J., Crisà, A., Ponce De León, F. A., … Smith, T. P. L.
593 (2017). Single-molecule sequencing and chromatin conformation capture enable de novo
594 reference assembly of the domestic goat genome. *Nature Genetics*, *49*(4), 643–650.
595 https://doi.org/10.1038/ng.3802
596 Bolger, A. M., Lohse, M., & Usadel, B. (2014). Trimmomatic: A flexible trimmer for Illumina
597 sequence data. *Bioinformatics*, *30*(15), 2114–2120.
598 https://doi.org/10.1093/bioinformatics/btu170
599 Borrill, P., Adamski, N., & Uauy, C. (2015). Genomics as the key to unlocking the polyploid
600 potential of wheat. In *New Phytologist* (Vol. 208, Issue 4, pp. 1008–1022).
601 https://doi.org/10.1111/nph.13533
602 Brandvain, Y., Kenney, A. M., Flagel, L., Coop, G., & Sweigart, A. L. (2014). Speciation and
603 introgression between Mimulus nasutus and Mimulus guttatus. *PLoS Genet*, *10*(6),
604 e1004410. https://doi.org/10.1371/journal.pgen.1004410

Burton, J. N., Adey, A., Patwardhan, R. P., Qiu, R., Kitzman, J. O., & Shendure, J. (2013). Chromosome-scale scaffolding of de novo genome assemblies based on chromatin interactions. *Nature Biotechnology*, *31*(12), 1119–1125. https://doi.org/10.1038/nbt.2727

Burton, T. L., & Husband, B. (2000). Fitness differences among diploids, tetraploids, and their triploid progeny in Chamerion angustifolium: Mechanisms of inviability and implications for polyploid evolution. *Evolution*, *54*(4), 1182–1191. https://doi.org/10.1111/j.0014-3820.2000.tb00553.x

Chen, Z. J., Sreedasyam, A., Ando, A., Song, Q., De Santiago, L. M., Hulse-Kemp, A. M., Ding, M., Ye, W., Kirkbride, R. C., Jenkins, J., Plott, C., Lovell, J., Lin, Y. M., Vaughn, R., Liu, B., Simpson, S., Scheffler, B. E., Wen, L., Saski, C. A., … Schmutz, J. (2020). Genomic diversifications of five Gossypium allopolyploid species and their impact on cotton improvement. *Nature Genetics*, *52*(5), 525–533. https://doi.org/10.1038/s41588-020-0614-5

Cheng, H., Concepcion, G. T., Feng, X., Zhang, H., & Li, H. (2021). Haplotype-resolved de novo assembly using phased assembly graphs with hifiasm. *Nature Methods*, *18*(2), 170–175. https://doi.org/10.1038/s41592-020-01056-5

Comai, L. (2005). The advantages and disadvantages of being polyploid. *Nature Reviews Genetics*, *6*(11), 836–846. https://doi.org/10.1038/nrg1711

Coughlan, J. M., Brown, M. W., & Willis, J. H. (2021). The genetic architecture and evolution of life-history divergence among perennials in the Mimulus guttatus species complex. *Proceedings of the Royal Society B: Biological Sciences*, *288*(1948). https://doi.org/10.1098/rspb.2021.0077

Coughlan, J. M., & Willis, J. H. (2019). Dissecting the role of a large chromosomal inversion in life history divergence throughout the Mimulus guttatus species complex. *Molecular Ecology*, *28*(6), 1343–1357. https://doi.org/10.1111/mec.14804

Coughlan, J. M., Wilson Brown, M., & Willis, J. H. (2020). Patterns of Hybrid Seed Inviability in the Mimulus guttatus sp. Complex Reveal a Potential Role of Parental Conflict in Reproductive Isolation. *Current Biology*, *30*(1), 83-93.e5. https://doi.org/10.1016/j.cub.2019.11.023

Coyne, J. A., & Orr, H. A. (2004). Speciation Sinauer Associates. *Sunderland, MA*, *276*, 281.

Danecek, P., Auton, A., Abecasis, G., Albers, C. A., Banks, E., DePristo, M. A., Handsaker, R. E., Lunter, G., Marth, G. T., Sherry, S. T., McVean, G., & Durbin, R. (2011). The variant call format and VCFtools. *Bioinformatics*, *27*(15), 2156–2158. https://doi.org/10.1093/bioinformatics/btr330

Danecek, P., Bonfield, J. K., Liddle, J., Marshall, J., Ohan, V., Pollard, M. O., Whitwham, A., Keane, T., McCarthy, S. A., & Davies, R. M. (2021). Twelve years of SAMtools and BCFtools. *GigaScience*, *10*(2). https://doi.org/10.1093/gigascience/giab008

Douglas, G. M., Gos, G., Steige, K. A., Salcedo, A., Holm, K., Josephs, E. B., Arunkumar, R., Ågren, J. A., Hazzouri, K. M., Wang, W., Platts, A. E., Williamson, R. J., Neuffer, B., Lascoux, M., Slotte, T., & Wright, S. I. (2015). Hybrid origins and the earliest stages of diploidization in the highly successful recent polyploid Capsella bursa-pastoris. *Proceedings of the National Academy of Sciences of the United States of America*, *112*(9), 2806–2811. https://doi.org/10.1073/pnas.1412277112

Doyle, J. J., Doyle, J. L., Brownt, A. H. D., Gracet, J. P., & Hortorium, L. H. B. (1990). *Multiple origins of polyploids in the Glycine tabacina complex inferred from chloroplast DNA polymorphism (restriction fragment variation/plant taxonomy)* (Vol. 87). https://www.pnas.org

651 Durand, N. C., Robinson, J. T., Shamim, M. S., Machol, I., Mesirov, J. P., Lander, E. S., &
652 Aiden, E. L. (2016). Juicebox Provides a Visualization System for Hi-C Contact Maps with
653 Unlimited Zoom. *Cell Systems*, *3*(1), 99–101. https://doi.org/10.1016/j.cels.2015.07.012
654 Edger, P. P., Poorten, T. J., VanBuren, R., Hardigan, M. A., Colle, M., McKain, M. R., Smith, R.
655 D., Teresi, S. J., Nelson, A. D. L., Wai, C. M., Alger, E. I., Bird, K. A., Yocca, A. E.,
656 Pumplin, N., Ou, S., Ben-Zvi, G., Brodt, A., Baruch, K., Swale, T., … Knapp, S. J. (2019).
657 Origin and evolution of the octoploid strawberry genome. *Nature Genetics*, *51*(3), 541–547.
658 https://doi.org/10.1038/s41588-019-0356-4
659 Faust, G. G., & Hall, I. M. (2014). SAMBLASTER: Fast duplicate marking and structural
660 variant read extraction. *Bioinformatics*, *30*(17), 2503–2505.
661 https://doi.org/10.1093/bioinformatics/btu314
662 Fishman, L., Kelly, A. J., & Willis, J. H. (2002). MINOR QUANTITATIVE TRAIT LOCI
663 UNDERLIE FLORAL TRAITS ASSOCIATED WITH MATING SYSTEM
664 DIVERGENCE IN MIMULUS. *Evolution*, *56*(11), 2138–2155.
665 https://doi.org/10.1111/j.0014-3820.2002.tb00139.x
666 Fishman, L., & Lila Fishman, M. (2020). 96-well CTAB-chloroform DNA extraction. *JUN*, *15*.
667 https://doi.org/10.17504/protocol
668 Fowler, N. L., & Levin, D. A. (2016). Critical factors in the establishment of allopolyploids.
669 *American Journal of Botany*, *103*(7), 1236–1251. https://doi.org/10.3732/ajb.1500407
670 Garner, A. G., Kenney, A. M., Fishman, L., & Sweigart, A. L. (2016). Genetic loci with parent-
671 of-origin effects cause hybrid seed lethality in crosses between Mimulus species. *New*
672 *Phytologist*, *211*(1), 319–331. https://doi.org/10.1111/nph.13897
673 Hegarty, M. J., Abbott, R. J., & Hiscock, S. J. (2012). Allopolyploid Speciation in Action: The
674 Origins and Evolution of Senecio cambrensis. In P. S. Soltis & D. E. Soltis (Eds.),
675 *Polyploidy and Genome Evolution* (pp. 245–270). Springer Berlin Heidelberg.
676 https://doi.org/10.1007/978-3-642-31442-1_13
677 Herben, T., Trávníček, P., & Chrtek, J. (2016). Reduced and unreduced gametes combine almost
678 freely in a multiploidy system. *Perspectives in Plant Ecology, Evolution and Systematics*,
679 *18*, 15–22. https://doi.org/10.1016/j.ppees.2015.12.001
680 Ivey, C. T., Habecker, N. M., Bergmann, J. P., Ewald, J., Frayer, M. E., & Coughlan, J. M.
681 (2023). Weak reproductive isolation and extensive gene flow between Mimulus glaucescens
682 and M. guttatus in northern California. *Evolution*, *77*(5), 1245–1261.
683 https://doi.org/10.1093/evolut/qpad044
684 Jakobsson, M., Hagenblad, J., Tavaré, S., Säll, T., Halldén, C., Lind-Halldén, C., & Nordborg,
685 M. (2006). A unique recent origin of the allotetraploid species Arabidopsis suecica:
686 Evidence from nuclear DNA markers. *Molecular Biology and Evolution*, *23*(6), 1217–1231.
687 https://doi.org/10.1093/molbev/msk006
688 Jiao, Y., Wickett, N. J., Ayyampalayam, S., Chanderbali, A. S., Landherr, L., Ralph, P. E.,
689 Tomsho, L. P., Hu, Y., Liang, H., Soltis, P. S., Soltis, D. E., Clifton, S. W., Schlarbaum, S.
690 E., Schuster, S. C., Ma, H., Leebens-Mack, J., & Depamphilis, C. W. (2011). Ancestral
691 polyploidy in seed plants and angiosperms. *Nature*, *473*(7345), 97–100.
692 https://doi.org/10.1038/nature09916
693 Kamal, N., Tsardakas Renhuldt, N., Bentzer, J., Gundlach, H., Haberer, G., Juhász, A., Lux, T.,
694 Bose, U., Tye-Din, J. A., Lang, D., van Gessel, N., Reski, R., Fu, Y. B., Spégel, P., Ceplitis,
695 A., Himmelbach, A., Waters, A. J., Bekele, W. A., Colgrave, M. L., … Sirijovski, N.

(2022). The mosaic oat genome gives insights into a uniquely healthy cereal crop. *Nature*, *606*(7912), 113–119. https://doi.org/10.1038/s41586-022-04732-y

Kenney, A. M., & Sweigart, A. L. (2016). Reproductive isolation and introgression between sympatric Mimulus species. *Molecular Ecology*, *25*(11), 2499–2517. https://doi.org/10.1111/mec.13630

Korunes, K. L., & Samuk, K. (2021). pixy: Unbiased estimation of nucleotide diversity and divergence in the presence of missing data. *Molecular Ecology Resources*, *21*(4), 1359–1368. https://doi.org/10.1111/1755-0998.13326

Kreiner, J. M., Kron, P., & Husband, B. C. (2017). Frequency and maintenance of unreduced gametes in natural plant populations: associations with reproductive mode, life history and genome size. *New Phytologist*, *214*(2), 879–889. https://doi.org/10.1111/nph.14423

Kryvokhyzha, D., Salcedo, A., Eriksson, M. C., Duan, T., Tawari, N., Chen, J., Guerrina, M., Kreiner, J. M., Kent, T. V, Lagercrantz, U., Stinchcombe, J. R., Glemin, S., Wright, S. I., & Lascoux, M. (2019). Parental legacy, demography, and admixture influenced the evolution of the two subgenomes of the tetraploid Capsella bursa-pastoris (Brassicaceae). *PLoS Genet*, *15*(2), e1007949. https://doi.org/10.1371/journal.pgen.1007949

Krzywinski, M., Schein, J., Birol, I., Connors, J., Gascoyne, R., Horsman, D., Jones, S. J., & Marra, M. A. (2009). Circos: an Information Aesthetic for Comparative Genomics. *Cold Spring Harbor Laboratory Press*. http://mkweb.bcgsc.ca/circos/tableviewer.

Leigh, J. W., & Bryant, D. (2015). POPART: Full-feature software for haplotype network construction. *Methods in Ecology and Evolution*, *6*(9), 1110–1116. https://doi.org/10.1111/2041-210X.12410

Levin, D. A. (1975). *Minority Cytotype Exclusion in Local Plant Populations* (Vol. 24, Issue 1).

Li, H. (2013). *Aligning sequence reads, clone sequences and assembly contigs with BWA-MEM*. http://arxiv.org/abs/1303.3997

Li, H. (2018). Minimap2: Pairwise alignment for nucleotide sequences. *Bioinformatics*, *34*(18), 3094–3100. https://doi.org/10.1093/bioinformatics/bty191

Li, H., & Durbin, R. (2010). Fast and accurate long-read alignment with Burrows-Wheeler transform. *Bioinformatics*, *26*(5), 589–595. https://doi.org/10.1093/bioinformatics/btp698

Lieberman-Aiden, E., Van Berkum, N. L., Williams, L., Imakaev, M., Ragoczy, T., Telling, A., Amit, I., Lajoie, B. R., Sabo, P. J., Dorschner, M. O., Sandstrom, R., Bernstein, B., Bender, M. A., Groudine, M., Gnirke, A., Stamatoyannopoulos, J., Mirny, L. A., Lander, E. S., & Dekker, J. (2009). Comprehensive mapping of long-range interactions reveals folding principles of the human genome. *Science*, *326*(5950), 289–293. https://doi.org/10.1126/science.1181369

Liu, J., Yao, Y., Xin, M., Peng, H., Ni, Z., & Sun, Q. (2022). Shaping polyploid wheat for success: Origins, domestication, and the genetic improvement of agronomic traits. *Journal of Integrative Plant Biology*, *64*(2), 536–563. https://doi.org/10.1111/jipb.13210

Lovell, J. T., Sreedasyam, A., Schranz, M. E., Wilson, M., Carlson, J. W., Harkess, A., Emms, D., Goodstein, D. M., & Schmutz, J. (2022). GENESPACE tracks regions of interest and gene copy number variation across multiple genomes. *ELife*, *11*.

Lowry, D. B., & Willis, J. H. (2010). A widespread chromosomal inversion polymorphism contributes to a major life-history transition, local adaptation, and reproductive isolation. *PLoS Biology*, *8*(9). https://doi.org/10.1371/journal.pbio.1000500

Lynch, M., & Force, A. G. (2000). The Origin of Interspecific Genomic Incompatibility via Gene Duplication. In *Am. Nat* (Vol. 156, Issue 6).

742 Martin, S. H., & Van Belleghem, S. M. (2017). Exploring evolutionary relationships across the
743 genome using topology weighting. *Genetics*, *206*(1), 429–438.
744 https://doi.org/10.1534/genetics.116.194720
745 Mavrodiev, E. V., Chester, M., Suárez-Santiago, V. N., Visger, C. J., Rodriguez, R., Susanna,
746 A., Baldini, R. M., Soltis, P. S., & Soltis, D. E. (2015). Multiple origins and chromosomal
747 novelty in the allotetraploid Tragopogon castellanus (Asteraceae). *New Phytologist*, *206*(3),
748 1172–1183. https://doi.org/10.1111/nph.13227
749 McKenna, A., Hanna, M., Banks, E., Sivachenko, A., Cibulskis, K., Kernytsky, A., Garimella,
750 K., Altshuler, D., Gabriel, S., Daly, M., & DePristo, M. A. (2010). The genome analysis
751 toolkit: A MapReduce framework for analyzing next-generation DNA sequencing data.
752 *Genome Research*, *20*(9), 1297–1303. https://doi.org/10.1101/gr.107524.110
753 Meimberg, H., Rice, K. J., Milan, N. F., Njoku, C. C., & McKay, J. K. (2009). Multiple origins
754 promote the ecological amplitude of allopolyploid Aegilops (Poaceae). *American Journal of*
755 *Botany*, *96*(7), 1262–1273. https://doi.org/10.3732/ajb.0800345
756 Michael, T. P., & VanBuren, R. (2020). Building near-complete plant genomes. In *Current*
757 *Opinion in Plant Biology* (Vol. 54, pp. 26–33). Elsevier Ltd.
758 https://doi.org/10.1016/j.pbi.2019.12.009
759 Modliszewski, J. L., & Willis, J. H. (2012). Allotetraploid Mimulus sookensis are highly
760 interfertile despite independent origins. *Mol Ecol*, *21*(21), 5280–5298.
761 https://doi.org/10.1111/j.1365-294X.2012.05706.x
762 Mower, J. P., Case, A. L., Floro, E. R., & Willis, J. H. (2012). Evidence against equimolarity of
763 large repeat arrangements and a predominant master circle structure of the mitochondrial
764 genome from a monkeyflower (Mimulus guttatus) lineage with cryptic CMS. *Genome*
765 *Biology and Evolution*, *4*(5), 670–686. https://doi.org/10.1093/gbe/evs042
766 Mukherjee, B. B., & Vickery, R. K. (1962). CHROMOSOME COUNTS IN THE SECTION
767 SIMIOLUS OF THE GENUS MIMULUS (SCROPHULARIACEAE). V. THE
768 CHROMOSOMAL HOMOLOGIES OF M. GUTTATUS AND ITS ALLIED SPECIES
769 AND VARIETIES. In *Source: Madroño* (Vol. 16, Issue 5).
770 https://www.jstor.org/stable/41423072?seq=1&cid=pdf-reference#references_tab_contents
771 Nelson, T. C., Stathos, A. M., Vanderpool, D. D., Finseth, F. R., Yuan, Y. W., & Fishman, L.
772 (2021). Ancient and recent introgression shape the evolutionary history of pollinator
773 adaptation and speciation in a model monkeyflower radiation (Mimulus section
774 Erythranthe). *PLoS Genetics*, *17*(2). https://doi.org/10.1371/journal.pgen.1009095
775 Nguyen, L. T., Schmidt, H. A., Von Haeseler, A., & Minh, B. Q. (2015). IQ-TREE: A fast and
776 effective stochastic algorithm for estimating maximum-likelihood phylogenies. *Molecular*
777 *Biology and Evolution*, *32*(1), 268–274. https://doi.org/10.1093/molbev/msu300
778 Novikova, P. Y., Hohmann, N., & Van de Peer, Y. (2018). Polyploid Arabidopsis species
779 originated around recent glaciation maxima. *Current Opinion in Plant Biology*, *42*, 8–15.
780 https://doi.org/10.1016/j.pbi.2018.01.005
781 Novikova, P. Y., Tsuchimatsu, T., Simon, S., Nizhynska, V., Voronin, V., Burns, R., Fedorenko,
782 O. M., Holm, S., Säll, T., Prat, E., Marande, W., Castric, V., Nordborg, M., & Irwin, D.
783 (2017). Genome sequencing reveals the origin of the allotetraploid arabidopsis suecica.
784 *Molecular Biology and Evolution*, *34*(4), 957–968. https://doi.org/10.1093/molbev/msw299
785 Ondov, B. D., Treangen, T. J., Melsted, P., Mallonee, A. B., Bergman, N. H., Koren, S., &
786 Phillippy, A. M. (2016). Mash: Fast genome and metagenome distance estimation using
787 MinHash. *Genome Biology*, *17*(1). https://doi.org/10.1186/s13059-016-0997-x

Oneal, E., Lowry, D. B., Wright, K. M., Zhu, Z., & Willis, J. H. (2014). Divergent population structure and climate associations of a chromosomal inversion polymorphism across the Mimulus guttatus species complex. *Molecular Ecology*, *23*(11), 2844–2860. https://doi.org/10.1111/mec.12778

Parks, D. H., Imelfort, M., Skennerton, C. T., Hugenholtz, P., & Tyson, G. W. (2015). CheckM: Assessing the quality of microbial genomes recovered from isolates, single cells, and metagenomes. *Genome Research*, *25*(7), 1043–1055. https://doi.org/10.1101/gr.186072.114

Penin, A. A., Kasianov, A. S., Klepikova, A. V, Omelchenko, D. O., Makarenko, M. S., & Logacheva, M. D. (2023). Origin and diversity of Capsella bursa-pastoris from the genomic point view. *BioRxiv*. https://doi.org/10.1101/2023.07.13.548917

Pont, C., Leroy, T., Seidel, M., Tondelli, A., Duchemin, W., Armisen, D., Lang, D., Bustos-Korts, D., Goué, N., Balfourier, F., Molnár-Láng, M., Lage, J., Kilian, B., Özkan, H., Waite, D., Dyer, S., Letellier, T., Alaux, M., Russell, J., … Çakır, E. (2019). Tracing the ancestry of modern bread wheats. *Nature Genetics*, *51*(5), 905–911. https://doi.org/10.1038/s41588-019-0393-z

Press, M. O., Wiser, A. H., Kronenberg, Z. N., Langford, K. W., Shakya, M., Lo, C.-C., Mueller, K. A., Sullivan, S. T., Chain, P. S. G., & Liachko, I. (n.d.). *Hi-C deconvolution of a human gut microbiome yields high-quality draft genomes and reveals plasmid-genome interactions*. https://doi.org/10.1101/198713

Puzey, J. R., Willis, J. H., & Kelly, J. K. (2017). Population structure and local selection yield high genomic variation in Mimulus guttatus. *Molecular Ecology*, *26*(2), 519–535. https://doi.org/10.1111/mec.13922

Ramsey, J. (2007). Unreduced gametes and neopolyploids in natural populations of Achillea borealis (Asteraceae). *Heredity*, *98*(3), 143–150. https://doi.org/10.1038/sj.hdy.6800912

Ramsey, J., & Schemske, D. W. (1998). PATHWAYS, MECHANISMS, AND RATES OF POLYPLOID FORMATION IN FLOWERING PLANTS. In *Annu. Rev. Ecol. Syst* (Vol. 29).

Rao, S. S. P., Huntley, M. H., Durand, N. C., Stamenova, E. K., Bochkov, I. D., Robinson, J. T., Sanborn, A. L., Machol, I., Omer, A. D., Lander, E. S., & Aiden, E. L. (2014). A 3D map of the human genome at kilobase resolution reveals principles of chromatin looping. *Cell*, *159*(7), 1665–1680. https://doi.org/10.1016/j.cell.2014.11.021

Razanajatovo, M., Maurel, N., Dawson, W., Essl, F., Kreft, H., Pergl, J., Pyšek, P., Weigelt, P., Winter, M., & Van Kleunen, M. (2016). Plants capable of selfing are more likely to become naturalized. *Nature Communications*, *7*. https://doi.org/10.1038/ncomms13313

Rodriguez, D. J. (1996). *A model for the establishment of polyploidy in plants*.

Scalabrin, S., Toniutti, L., Di Gaspero, G., Scaglione, D., Magris, G., Vidotto, M., Pinosio, S., Cattonaro, F., Magni, F., Jurman, I., Cerutti, M., Suggi Liverani, F., Navarini, L., Del Terra, L., Pellegrino, G., Ruosi, M. R., Vitulo, N., Valle, G., Pallavicini, A., … Bertrand, B. (2020). A single polyploidization event at the origin of the tetraploid genome of Coffea arabica is responsible for the extremely low genetic variation in wild and cultivated germplasm. *Scientific Reports*, *10*(1). https://doi.org/10.1038/s41598-020-61216-7

Segraves, K. A., Thompson, J. N., Soltis, P. S., & Soltis, D. E. (1999). Multiple origins of polyploidy and the geographic structure of Heuchera grossulariifolia. *Molecular Ecology*, *8*(2), 253–262. https://doi.org/10.1046/j.1365-294X.1999.00562.x

Shumate, A., & Salzberg, S. L. (2021). Liftoff: Accurate mapping of gene annotations. *Bioinformatics*, *37*(12), 1639–1643. https://doi.org/10.1093/bioinformatics/btaa1016

Sigel, E. M., Windham, M. D., & Pryer, K. M. (2014). Evidence for reciprocal origins in Polypodium hesperium (Polypodiaceae): A fern model system for investigating how multiple origins shape allopolyploid genomes. *American Journal of Botany*, *101*(9), 1476–1485. https://doi.org/10.3732/ajb.1400190

Simão, F. A., Waterhouse, R. M., Ioannidis, P., Kriventseva, E. V., & Zdobnov, E. M. (2015). BUSCO: Assessing genome assembly and annotation completeness with single-copy orthologs. *Bioinformatics*, *31*(19), 3210–3212. https://doi.org/10.1093/bioinformatics/btv351

Slotte, T., Ceplitis, A., Neuffer, B., Hurka, H., & Lascoux, M. (2006). Intrageneric phylogeny of Capsella (Brassicaceae) and the origin of the tetraploid C. bursa-pastoris based on chloroplast and nuclear DNA sequences. *American Journal of Botany*, *93*(11), 1714–1724. https://doi.org/10.3732/ajb.93.11.1714

Soltis, D. E., & Soltis, P. S. (1999). *Polyploidy: recurrent formation and genome evolution* (Vol. 14, Issue 9).

Soltis, D. E., Visger, C. J., Blaine Marchant, D., & Soltis, P. S. (2016). Polyploidy: Pitfalls and paths to a paradigm. *American Journal of Botany*, *103*(7), 1146–1166. https://doi.org/10.3732/ajb.1500501

Soltis, D. E., Visger, C. J., & Soltis, P. S. (2014). The polyploidy revolution then...and now: Stebbins revisited. *American Journal of Botany*, *101*(7), 1057–1078. https://doi.org/10.3732/ajb.1400178

Soltis, P. S., & Soltis, D. E. (1991). *Multiple Origins of the Allotetraploid Tragopogon mirus (Compositae): rDNA Evidence*. *16*(3), 407–413.

Stewart, R. D., Auffret, M. D., Warr, A., Wiser, A. H., Press, M. O., Langford, K. W., Liachko, I., Snelling, T. J., Dewhurst, R. J., Walker, A. W., Roehe, R., & Watson, M. (2018). Assembly of 913 microbial genomes from metagenomic sequencing of the cow rumen. *Nature Communications*, *9*(1). https://doi.org/10.1038/s41467-018-03317-6

Sweigart, A. L., Martin, N. H., & Willis, J. H. (2008). Patterns of nucleotide variation and reproductive isolation between a Mimulus allotetraploid and its progenitor species. *Mol Ecol*, *17*(8), 2089–2100. https://doi.org/10.1111/j.1365-294X.2008.03707.x

Sweigart, A. L., & Willis, J. H. (2003). Patterns of nucleotide diversity in two species of Mimulus are affected by mating system and asymmetric introgression. *Evolution*, *57*(11), 2490–2506. https://doi.org/10.1111/j.0014-3820.2003.tb01494.x

Vallejo-Marín, M., Buggs, R. J. A., Cooley, A. M., & Puzey, J. R. (2015). Speciation by genome duplication: Repeated origins and genomic composition of the recently formed allopolyploid species Mimulus peregrinus. *Evolution*, *69*(6), 1487–1500. https://doi.org/10.1111/evo.12678

Vallejo-Marín, M., Cooley, A. M., Lee, M. Y., Folmer, M., McKain, M. R., & Puzey, J. R. (2016). Strongly asymmetric hybridization barriers shape the origin of a new polyploid species and its hybrid ancestor. *American Journal of Botany*, *103*(7), 1272–1288. https://doi.org/10.3732/ajb.1500471

Vickery, R. K. (1978). Case Studies in the Evolution of Species Complexes in Mimulus. In W. C. and W. B. Hecht Max K. and Steere (Ed.), *Evolutionary Biology* (pp. 405–507). Springer US. https://doi.org/10.1007/978-1-4615-6956-5_7

Vickery, R. K. (1995). Speciation by aneuploidy and polyploidy in Mimulus (Scrophulariaceae). In *Brigham Young University SPECIATION BY ANEUPLOIDY AND POLYPLOIDY IN*

MIMULUS (SCROPHULARIACEAE) Source: The Great Basin Naturalist (Vol. 55, Issue 2).

Wickham H. (2016). *ggplot2: Elegant Graphics for Data Analysis.* Springer-Verlag New York.

Wolfe, T. M., Balao, F., Trucchi, E., Bachmann, G., Gu, W., Baar, J., Hedrén, M., Weckwerth, W., Leitch, A. R., & Paun, O. (2023). Recurrent allopolyploidizations diversify ecophysiological traits in marsh orchids (*Dactylorhiza majalis* s.l.). *Molecular Ecology*, *32*(17), 4777–4790. https://doi.org/10.1111/mec.17070

Wood, D. E., Lu, J., & Langmead, B. (2019). Improved metagenomic analysis with Kraken 2. *Genome Biology*, *20*(1). https://doi.org/10.1186/s13059-019-1891-0

Wright, S. I., Kalisz, S., & Slotte, T. (2013). Evolutionary consequences of self-fertilization in plants. In *Proceedings of the Royal Society B: Biological Sciences* (Vol. 280, Issue 1760). Royal Society. https://doi.org/10.1098/rspb.2013.0133

Zheng, X., Levine, D., Shen, J., Gogarten, S. M., Laurie, C., & Weir, B. S. (2012). A high-performance computing toolset for relatedness and principal component analysis of SNP data. *Bioinformatics*, *28*(24), 3326–3328. https://doi.org/10.1093/bioinformatics/bts606

Zou, X. H., Du, Y. S., Tang, L., Xu, X. W., Doyle, J. J., Sang, T., & Ge, S. (2015). Multiple origins of BBCC allopolyploid species in the rice genus (Oryza). *Scientific Reports*, *5*. https://doi.org/10.1038/srep14876

Zuellig, M. P., & Sweigart, A. L. (2018). Gene duplicates cause hybrid lethality between sympatric species of Mimulus. *PLoS Genetics*, *14*(4). https://doi.org/10.1371/journal.pgen.1007130

Figure legends

Table 1: The *M. sookensis* genome can be split into two distinct subgenomes based on similarity to *M. nasutus* SF. SD: Standard deviation.

Figure 1: *M. sookensis* shows high levels of synteny with diploid relatives *M. nasutus* and *M. guttatus.* Genespace syntenic map created using the *M. sookensis* v1, *M. guttatus* v3, and *M. nasutus* v1 reference genomes.

Figure 2: *M. sookensis* populations show little genetic structure in a PCA. PC1 and PC2 explain 19.21% and 15.01% of the variation respectively. Samples collected from Vancouver Island, BC, Canada are shown by circles and those collected from Oregon, USA are shown by triangles. Sample locations are shown in map on left (note one population has two accessions).

Figure 3: Maximum likelihood tree of *M. sookensis* subgenomes and diploid relatives in the *M. guttatus* species complex. The ML tree was generated in IQ Tree using the TVM + F + R2 model from 1,711,738 parsimony informative sites with *M. dentilobus* as an outgroup.

Figure 4: Genome-wide TWISST weightings quantifying support for one or more diploid species as the closest relative to *M. sookensis* subgenome B. Data are from 16,754 rooted gene trees with five “species” (subgenome B, *M. decorus*, northern *M. guttatus*, southern *M. guttatus*,

and subgenome A + *M. nasutus*) plus *M. dentilobus* (not shown) as the outgroup. (A) The 105 topologies were grouped into 15 simplified classes (A-O) defined by which diploid species (or combination) is most closely related (i.e., sister) to *M. sookensis* subgenome B (indicated with gray shading). Frequencies of each topology class are given to the right of the table; the whole-genome species tree is depicted at the top. (B) The top three topology classes.

Figure 5: **Haplotype networks of organellar genomic variation point to *M. nasutus* as the maternal progenitor of *M. sookensis*.** (A) Chloroplast haplotype network generated using 91 parsimony-informative sites. (B) Mitochondrial haplotype network generated using 100 parsimony-informative sites. Haplotypes represented by more than one sample are indicated with numbers (individual samples in numbered groups are listed below each network).

Figure S1: Range map of species used in this study. Hand-drawn **r**anges are based on both sampled locations as well as observations and herbarium records. *M. sookensis* and *M. decorus* can be easily mis-identified as *M. nasutus* and *M. guttatus* respectively so ranges are an approximation.

Table S1: Population sample information of all lines used in this study. Depth for each line was calculated when mapped to the *M. guttatus* hardmasked v5 genome or to the *M. sookensis* FAN v1 genome.

Table S2: Nucleotide diversity and divergence of focal species. *Dxy* and π between *M. sookensis* subgenomes (A and B), *M. nasutus* (N), and *M. guttatus* (G) calculated on fourfold degenerate sites.

Figure S2 – *M. sookensis* contains 28 primary scaffolds. Heatmap generated from HiC data and used to scaffold *M. sookensis* contigs. Scaffold identities are listed below x-axis.

Figure S3: Homology between *M. sookensis* and its two progenitors. A. *M. sookensis* v1.0 reference genome mapped to the *M. guttatus* v3 IM62 reference genome. Each *M. guttatus* chromosome shows homology with 2 *M. sookensis* chromosomes. Each dot indicates 75 Kb of homology. **B**. *M. sookensis* v1reference mapped against the *M. nasutus* v1 reference. Each *M. nasutus* chromosome shows homology with two *M. sookensis* chromosomes. Scaffolds are ordered from largest to smallest in size.

Figure S4: M. sookensis subgenomes show high homology between subgenomes. Circos plot generated from regions of homology between subgenomes A and B. Single ribbons represent 10 Kb regions of homology with a mapping quality of 60.

Figure S5: NJ tree generated from 14,000 SNPs, bootstrapped 1000 times.

Figure S6: Maximum likelihood tree of *M. sookensis* subgenomes and diploid relatives in the *M. guttatus* species complex. The ML tree was generated in IQ Tree using the TVM + F + R2 model from 1,711,738 parsimony informative sites with *M. dentilobus* as an outgroup.

Figure S7: TWISST topology weights for gene trees with three "species": *M. decorus*, northern *M. guttatus*, and southern *M. guttatus* + *M. nasutus*. Data are from 16,754 gene trees rooted by *M. dentilobus* (not shown).

Figure S8: All 15 simplified TWISST topology classes. Letters correspond to Figure 4.

Figure S9: Distribution of top three simplified TWISST topology classes across the 14 chromosomes. Topologies were summed across windows of nine genes and plotted across the genome. Topology A is shown in green, Topology B in light blue, and topology C in navy.

Figure S10: Distribution of the fourth most common TWISST topology class across the 14 chromosomes. Topology D, which places *M. sookensis* subgenome B sister to *M. nasutus* + subgenome A could indicate regions of homoeologous recombination or gene conversion between subgenomes. Weights of topology D were summed across windows of 9 genes. Weightings are indicative of proportion of topology D in comparison to all other topologies.

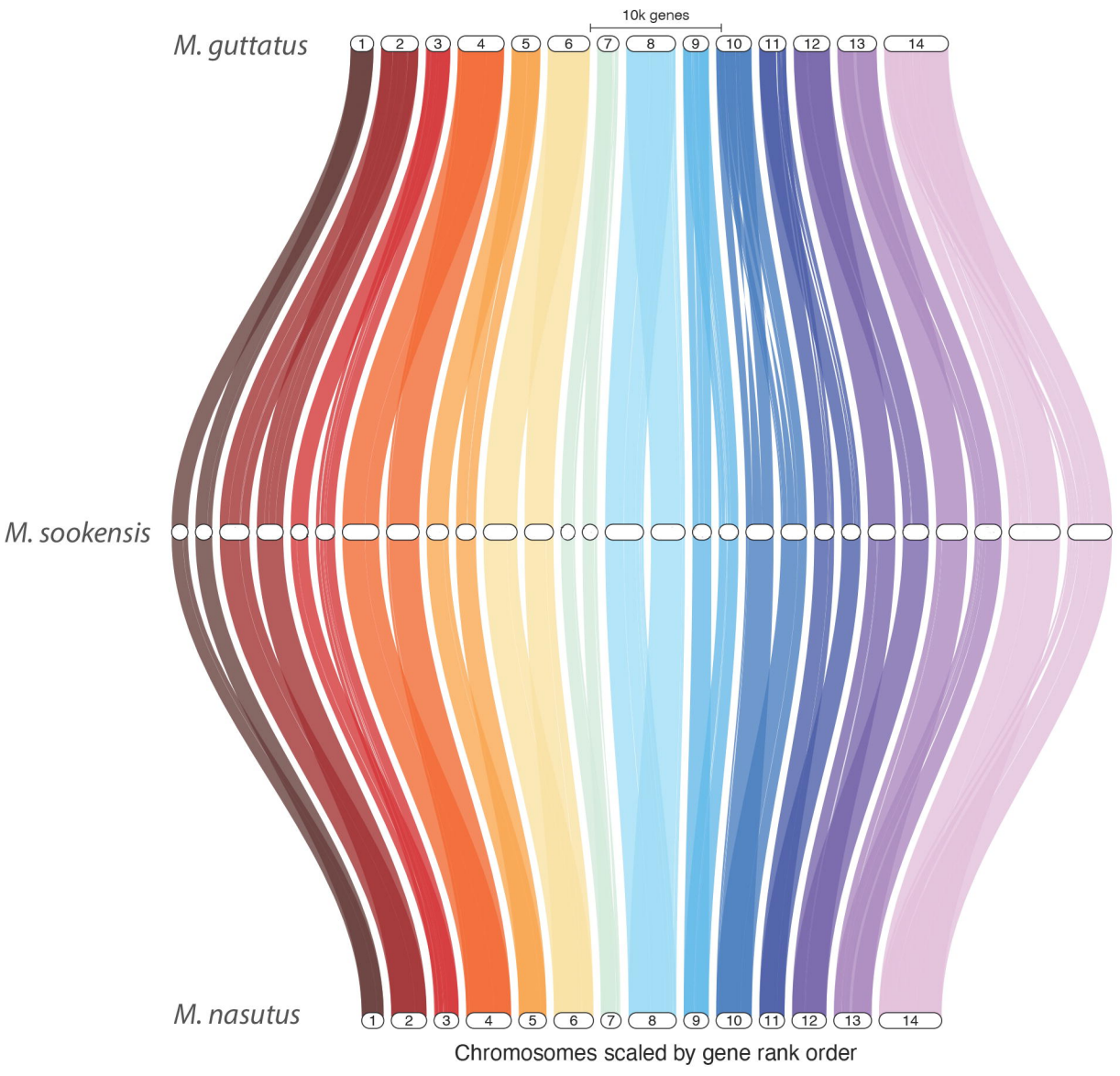
10k genes
M. guttatus
1
2
3
4
5
6
7
8
9
10
11
12
13
14
M. sookensis
M. nasutus
1
2
3
4
5
6
7
8
9
10
11
12
13
14
Chromosomes scaled by gene rank order

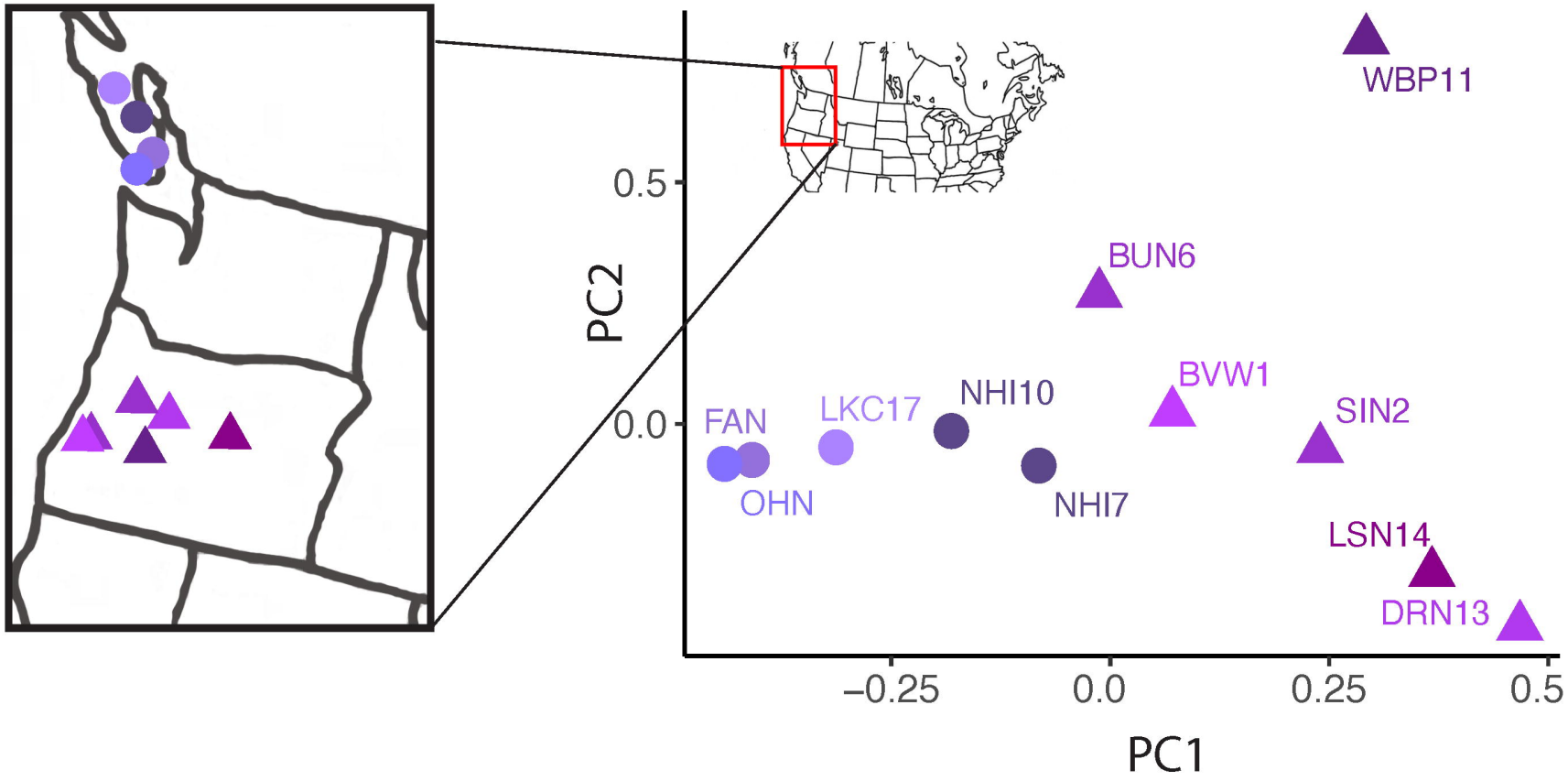
WBP11
BUN6
BVW1
SIN2
NHI10
LKC17
FAN
OHN
NHI7
LSN14
DRN13
0.5
0.0
PC2
−0.25
0.0
0.25
0.5
PC1

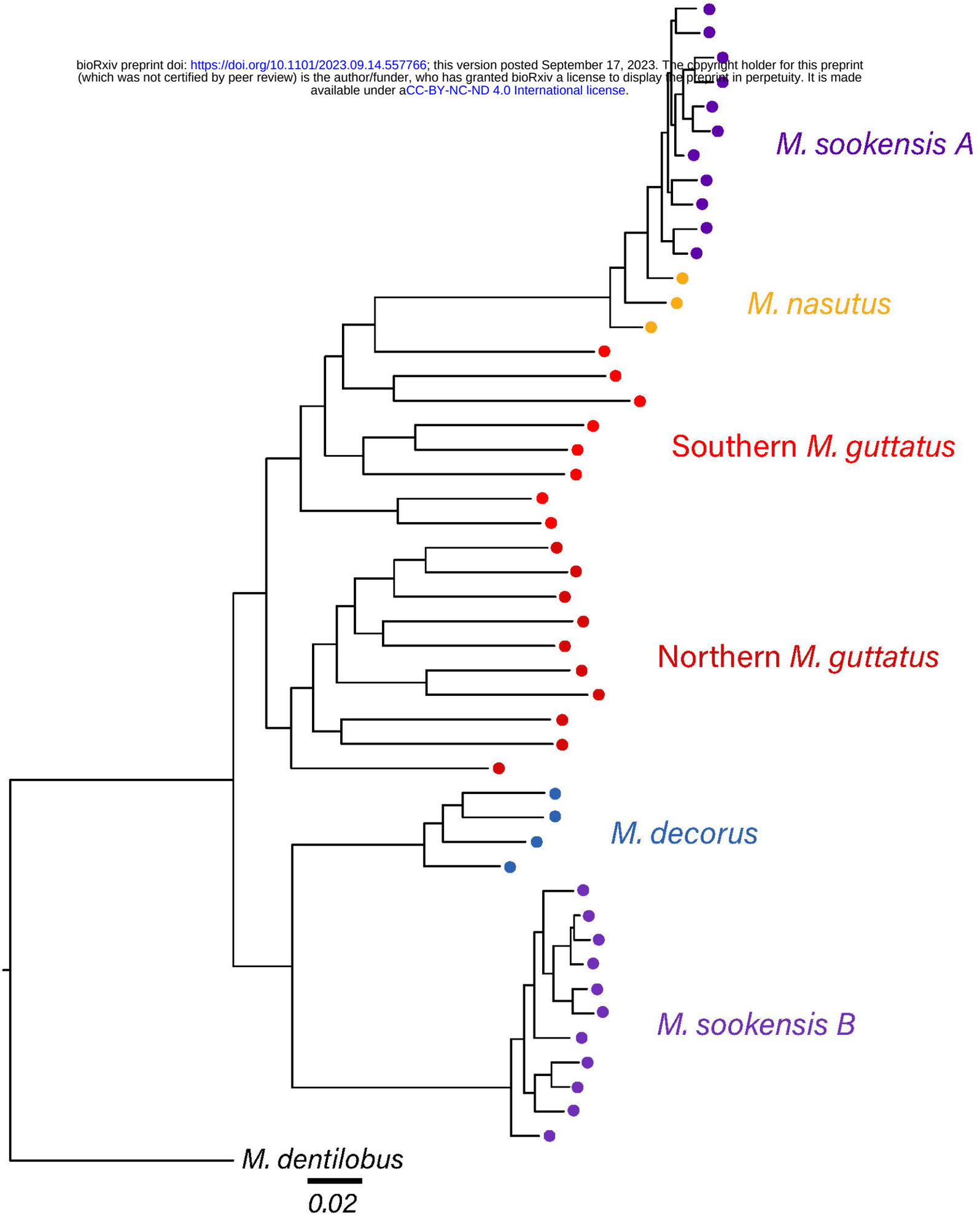

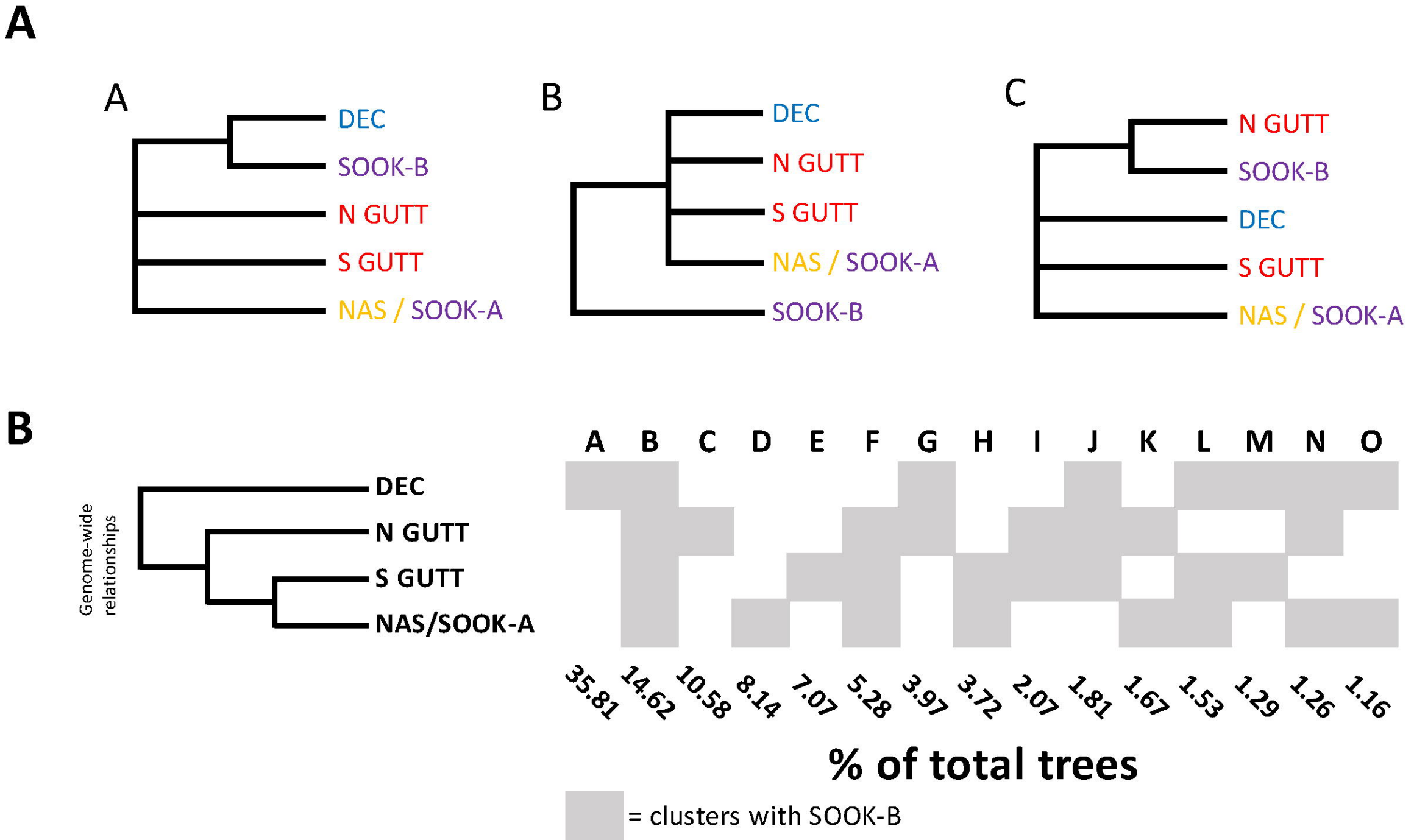
A
A
DEC
SOOK-B
N GUTT
S GUTT
NAS / SOOK-A
B
DEC
N GUTT
S GUTT
NAS / SOOK-A
SOOK-B
C
N GUTT
SOOK-B
DEC
S GUTT
NAS / SOOK-A
B
Genome-wide relationships
DEC
N GUTT
S GUTT
NAS/SOOK-A
A B C D E F G H I J K L M N O
35.81 14.62 10.58 8.14 7.07 5.28 3.97 3.72 2.07 1.81 1.67 1.53 1.29 1.26 1.16
% of total trees
= clusters with SOOK-B

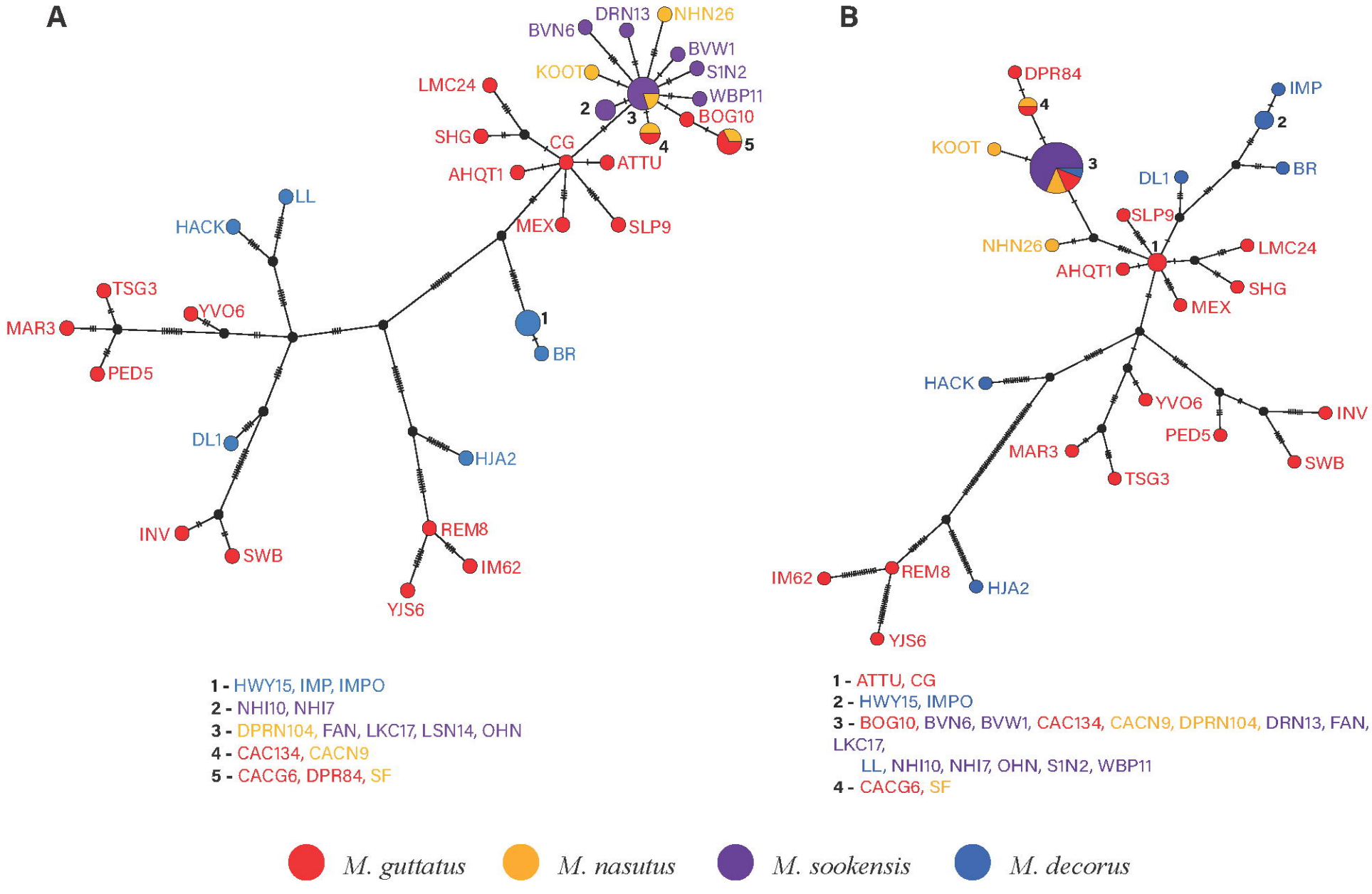
A
DRN13
NHN26
BVN6
BVW1
KOOT
S1N2
LMC24
WBP11
2
3
BOG10
4
5
SHG
CG
ATTU
AHQT1
LL
HACK
MEX
SLP9
TSG3
YVO6
MAR3
1
BR
PED5
DL1
HJA2
INV
REM8
SWB
IM62
YJS6
1 - HWY15, IMP, IMPO
2 - NHI10, NHI7
3 - DPRN104, FAN, LKC17, LSN14, OHN
4 - CAC134, CACN9
5 - CACG6, DPR84, SF
B
DPR84
4
IMP
2
KOOT
3
BR
DL1
SLP9
NHN26
1
LMC24
AHQT1
SHG
MEX
HACK
YVO6
INV
PED5
MAR3
SWB
TSG3
IM62
REM8
HJA2
YJS6
1 - ATTU, CG
2 - HWY15, IMPO
3 - BOG10, BVN6, BVW1, CAC134, CACN9, DPRN104, DRN13, FAN, LKC17,
LL, NHI10, NHI7, OHN, S1N2, WBP11
4 - CACG6, SF
M. guttatus
M. nasutus
M. sookensis
M. decorus